Quantum Electronics **50** (3) 267–271 (2020)

https://doi.org/10.1070/QEL17258

Frequency transfer via an ultra-stable free-space link

K.S. Kudeyarov, D.S. Kryuchkov, G.A. Vishnyakova, N.O. Zhadnov,
K.Yu. Khabarova, N.N. Kolachevsky

Abstract. **An optical frequency transfer at a wavelength of 1542 nm via an ultra-stable 5-m free-space link with active compensation of the phase noise caused by atmospheric fluctuations is demonstrated. The link-induced phase noise and its contribution to the frequency transfer instability are investigated. It is shown that, with the phase compensation system switched on, the link contribution to the relative transfer instability in terms of Allan deviation reaches 1.7×10^{-19} for a 5000-s averaging time.**

Keywords: *optical frequency transfer, relative frequency instability, Allan deviation, power spectral density of phase noise, free-space link, atmospheric turbulence.*

1. Introduction

The elaboration of a network of optical clocks connected with links for coherent transfer of frequency and time signals opens up great possibilities for developing such fields of science and technology as the formation of national and international time scales [1], satellite navigation [2], relativistic geodesy [3], very-long-baseline interferometry [4], tests of fundamental theories [5], and search for dark matter [6]. The modern frequency standards have reached the level of relative uncertainty and instability of 10^{-18} [7, 8]. Signals from these standards cannot be transferred with conservation of their characteristics using radio frequency (RF) methods, because the latter cannot provide frequency transfer instability better than 10^{-16} [9]. Transferring signals at optical frequencies, one can reduce the level of the phase noise introduced by the communication link. Due to the active development of methods for transferring highly stable signals through fibre links in the last decade, coherent frequency transfer at distances of up to 2000 km [10] and time signal transfer at a distance of 6000 km [11] have been implemented. At the same time, communication with transported standards (which may be located beyond the fibre infrastructure zone) is necessary for many applications; hence, free-space optical links must be formed. Furthermore, these links can be used for clock synchronisation between ground-based stations and satellites [12]. The joint use of fibre and free-space communication links will make it possible to develop a global network for transferring precise frequency and time signals.

The stability and accuracy of a signal transferred through a free-space link can be limited by the atmospheric turbulence, which affects both the amplitude and phase of a light signal. Fluctuations of the refractive index of air introduce perturbations (Doppler noise) into the signal phase; the spectrum of this noise is described by the Kolmogorov theory of turbulence [13]. According to this theory, the power spectral density of phase noise is

$$S_\varphi(f) = 0.016k^2C_n^2LV^{5/3}f^{-8/3}, \quad (1)$$

where f is frequency, k is the wave number of light, C_n is the atmospheric turbulence structure constant, L is the free-space link length, and V is the wind speed.

Different methods of compensating for introduced perturbations are used to preserve the characteristics of transferred signals. The O-TWTFT method, which is based on two-way exchange with femtosecond comb pulses, makes it possible to transfer a frequency signal with a relative instability at a level of 10^{-18} and synchronise time with femtosecond accuracy at a link length up to 4 km [14]. However, the complexity and high cost of such systems is a hindrance for their installation on transportable objects. A possible alternative solution is the frequency transfer methods with application of cw lasers, by analogy with the technique used in fibre links. A frequency transfer at a distance of 600 m with a relative instability of 1.3×10^{-18} for an averaging time of 64 s was demonstrated in [15]. A further increase in the free-space link length calls for additional consideration of some atmospheric effects. To compensate for the laser beam path distortions in an open-air link, which affect the transferred radiation collection efficiency, one needs a system for active adjustment of the beam direction [16]. In addition, the wavefront distortion (described by the Fried parameter [17]) does not make it possible to increase the laser beam size in order to reduce divergence at large distances. The wavefront distortions can be compensated using adaptive optics [18]. The problem of transferring high-precision signals to a mobile object remains unsolved.

The development of stationary and transportable optical frequency standards in Russia [19–21] shows the necessity of designing both fibre and free-space links for the transfer of highly stable signals. A signal transfer through fibre links has successfully been implemented under laboratory conditions

K.S. Kudeyarov, D.S. Kryuchkov, G.A. Vishnyakova, N.O. Zhadnov Lebedev Physical Institute, Russian Academy of Sciences, Leninsky prosp. 53, 119991 Moscow, Russia; e-mail: gulnarav7@gmail.com;
K.Yu. Khabarova All-Russian Scientific Research Institute of Physical-Technical and Radiotechnical Measurements (VNIIFTRI), 141570 Mendeleevo, Moscow region, Russia;
N.N. Kolachevsky Lebedev Physical Institute, Russian Academy of Sciences, Leninsky prosp. 53, 119991 Moscow, Russia; Russian Quantum Center, Bol'shoi bul'var 30, stroenie 1, Skolkovo, 121205 Moscow, Russia

Received 4 February 2020
Kvantovaya Elektronika **50** (3) 267–271 (2020)
Translated by Yu.P. Sin'kov

[22]. At the same time, the transfer via open-air links has not been investigated yet. In this paper we report the results of developing a laboratory 5-m link with a system for active compensation of phase noise and studying the attainable relative frequency instability and uncertainty.

2. Experimental setup

A schematic of the experiment is shown in Fig. 1. The phase noise introduced by the link is detected using an autoheterodyning circuit [22], in which a beam of 1542-nm Koheras ADJUSTIK fibre laser passes through an acousto-optic modulator (AOM), controlled by an RF generator G1 at a frequency of 38.4 MHz. Two beam passes (in the forward and backward directions) lead to the formation of an inloop beat signal with a reference beam on the photodiode PD1 at the sender side; this signal contains information about the noise phase. The radiation power after the first pass through the AOM is 13 mW, the return radiation power on the photodiode is 0.3 mW, and the reference radiation power is 1 mW. The photodiode signal is mixed on an analogue phase detector (double balance mixer) with the signal from reference RF generator G2 at a frequency of 76.8 MHz to form an error signal in the feedback loop, which, in turn, is applied to a proportional-integral amplifier (PIA) based on a field-programmable gate array board STEMlab Red Pitaya. The output signal from the PIA arrives at the frequency-modulation (FM) input of RF generator G1, which feeds the AOM, and thus compensates for the signal phase fluctuations.

At the receiver side of the link, some part of radiation is split off by a polarising beam splitter (cube) and essentially is a signal delivered to a distant user. The rest of radiation is reflected back by a mirror to form a inloop signal. The beam splitter and mirror are fixed on a common base. It can be shown [23] that, strictly speaking, for a closed feedback loop, the accuracy and stability characteristics of the transferred and return signals may differ. In addition, the noise suppression efficiency depends on the identity degree of noises introduced by the link during the forward and backward beam propagation is satisfied. Therefore, to perform a comprehensive analysis of the link performance, a remote user is ususally located close to the sender side to allow for another (remote) beat signal formation (see Fig. 1). The powers of the transferred and reference beams on photodiode PD2 are, respectively, 0.9 and 2 mW. The parameters of this signal belong to the most important operational characteristics of the system. An alternative way is to use another (similar) link equipped with a noise compensation system to return the signal received

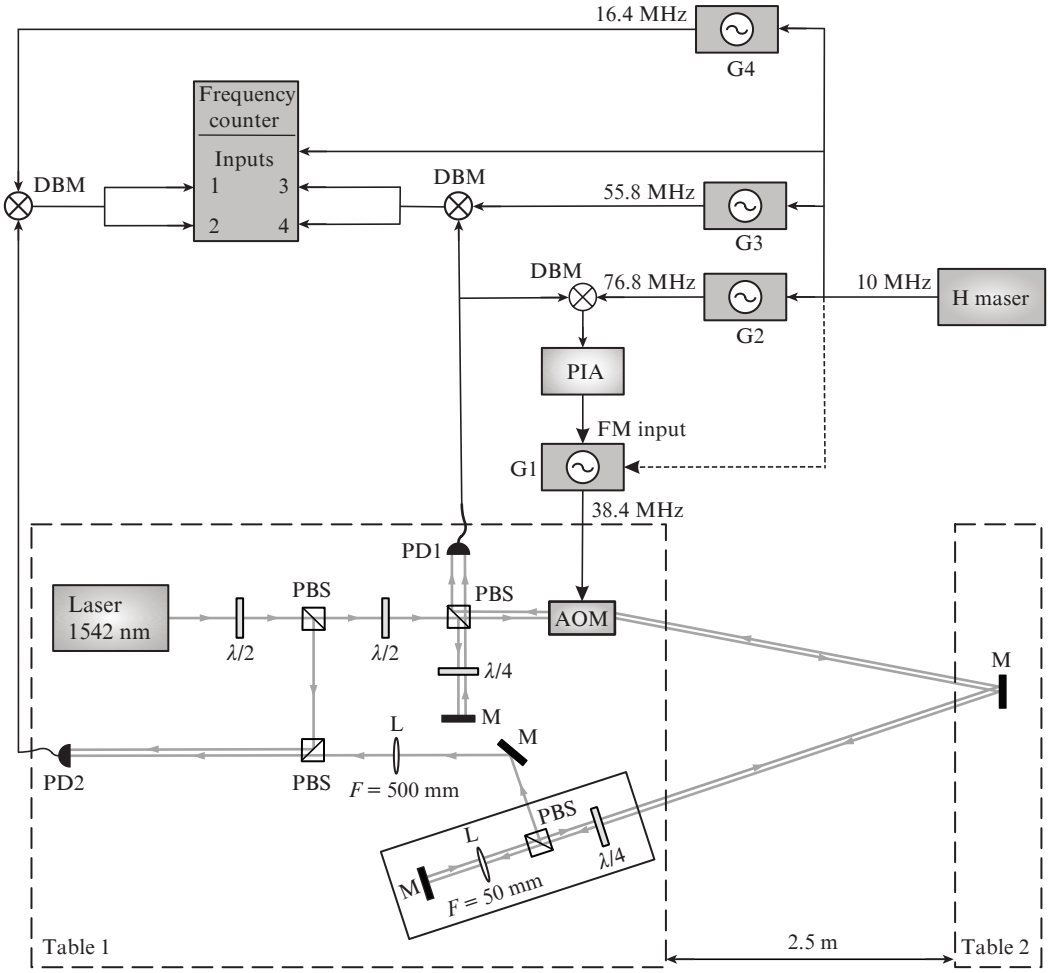

Figure 1. Schematic of the experimental setup:
(AOM) acousto-optic modulator; (PD1, PD2) photodiodes measuring the inloop and remote signals, respectively; (PIA) proportional-integral amplifier; ($\lambda/2, \lambda/4$) half- and quarter-wave phase plates, respectively; (G1 – G4) RF generators; (FM) frequency-modulation input of RF generator; (H maser) passive hydrogen maser; (M) mirror; (PBS) polarising beam splitter; (L) lens; (DBM) double balanced mixer.

by a remote user is returned to the sender side to form a remote beat signal (the so-called antiparallel scheme).

The length of the link under study is 5 m. All optical elements of the circuit, except for one mirror, are installed on the same optical table, whereas the mirror (located at a distance of about the link half-length) is mounted on another table (Fig. 1). This configuration is closer to real conditions, in which the receiving side is not completely immobile.

A high-resolution dead-time-free frequency counter K + K Messtecknik, operating in the Λ (phase averaging) mode, is used to measure the signal beat frequencies. The beat signals are amplified, mixed in double balanced mixers with signals from RF generators G3 and G4 in order to obtain convenient frequency ranges, and filtered; then each beat signal is fed into two counter channels to determine possible cycle slip events. Only the data stretches free of cycle slips are taken into account in the analysis. A 10-MHz signal from a passive hydrogen maser is applied to the reference inputs of all RF generators and counter. Note that the maser is not a necessary element in this experiment; it is sufficient to use the 10-MHz signal from the RF generator. Generator G1 needs a 10-MHz reference signal only when analysing the link in the absence of noise compensation. The counter data are used to calculate the mean frequencies; the Allan deviation σ_y, where $y = \Delta\nu(t)/\nu_0$ are the relative frequency fluctuations, ν_0 is the carrier optical frequency (194 THz for λ = 1542 nm); and the power spectral density of phase noise, $S_\varphi(f)$. These characteristics allow one to draw conclusions about the signal inaccuracy and instability, as well as about the character of dominant noises [24].

3. Results and discussion

Figure 2 shows time dependences of the frequencies of inloop and remote beat signals, measured with a counter window of 1 ms. The feedback loop was switched on at t = 86 s. One can clearly see a decrease in frequency fluctuations. Figure 3 presents the relative frequency instability in terms of Allan deviation for inloop and remote signals obtained in four measurement series: in the absence of noise compensation (upper curves), with 1-ms and 1-s counter measurement windows, and with a feedback loop switched on (lower curves), with 1-ms and 1-s windows. The measurement time for the 1-s window was 37 000 s.

The noise compensation system makes it possible to suppress the contribution of the link to the transferred signal instability from 1.8×10^{-15} to 2.2×10^{-16} for an averaging time of 1 s and from 1.6×10^{-18} to 1.7×10^{-19} for a time of 5000 s. The contribution to the uncertainty (deviation of the mean from the nominal value) after the 37000-s averaging decreases from 1 mHz to 25 μHz or from 5×10^{-18} to 1.25×10^{-19} in relative units. These characteristics are quite appropriate to use this link when comparing the best modern transportable frequency standards [25]. In the case of inloop signal, the contribution to instability decreases from 3.6×10^{-15} to 7.3×10^{-19} for a time of 1 s and from 2.8×10^{-18} to 7.7×10^{-22} for a time of 5000 s; the contribution to the frequency inaccuracy increases from 1.4 mHz to 50 nHz or from 7×10^{-18} to 2.5×10^{-22}, respectively. The characteristics of the inloop signal are much better than those of the remote one; the possible reasons are discussed below.

Based on the character of the dependence of deviation on the averaging time one can draw conclusions about the type of dominant noise; however, this is difficult to do in the case of a complex noise structure. To gain a deeper insight into the nature of noise, it is convenient to consider the power spectral density of phase noise, $S_\varphi(f)$. Figure 4 shows the power spectral density of phase noise, constructed based on series of data obtained with a 1-ms counter window.

An approximation of uncompensated data on signals in the frequency range of 0.1–10 Hz by a power-law function yields the least error for a power of –2.3 [i.e., $S_\varphi(f) \backsim f^{-2.3}$]; this indicates the dominance of noise caused by air turbulence. Deviations from the Kolmogorov spectrum (described by the function $f^{-8/3}$) were repeatedly observed in various experiments (in particular, the dependence $f^{-2.3}$ was recorded in [13] when transferring signals by the O-TWTFT method via open-air street links). Formula (1) allows one to estimate the turbulence structure constant C_n for a link studied: on the assumption that the velocity of the air motion caused by the

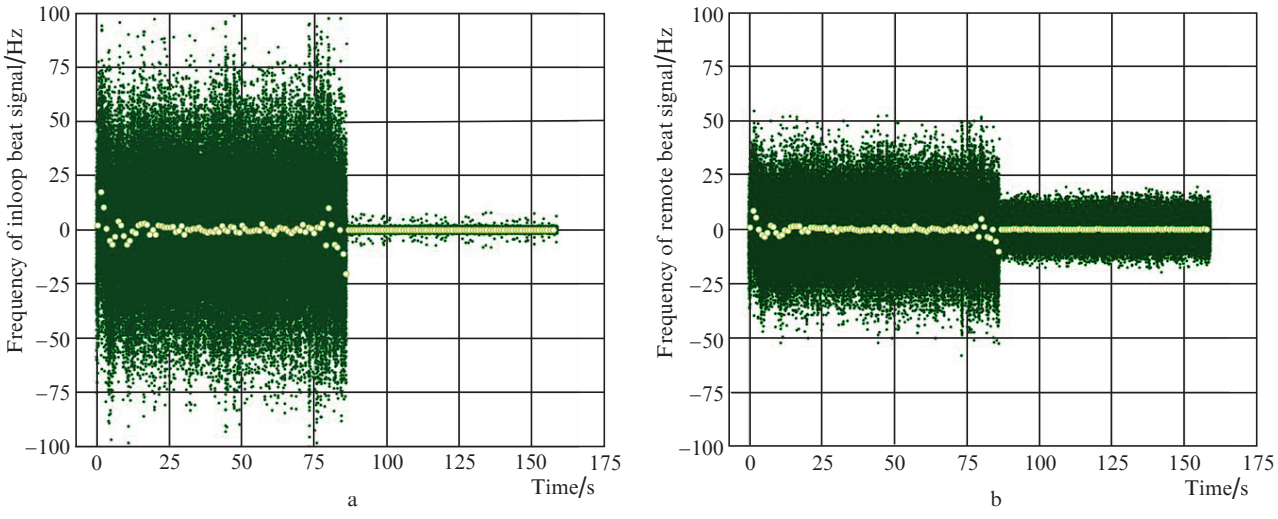

Figure 2. Time dependences of the frequencies of (a) inloop and (b) remote beat signals. The feedback loop was activated at the instant t = 86 s. The field of dark dots is a set of data obtained with a counter measurement window of 1 ms; the bright dots are the data after 1-s averaging. For clarity, the frequencies of the inloop and remote beat signals are shown with subtracted 21 and 22 MHz values, respectively.

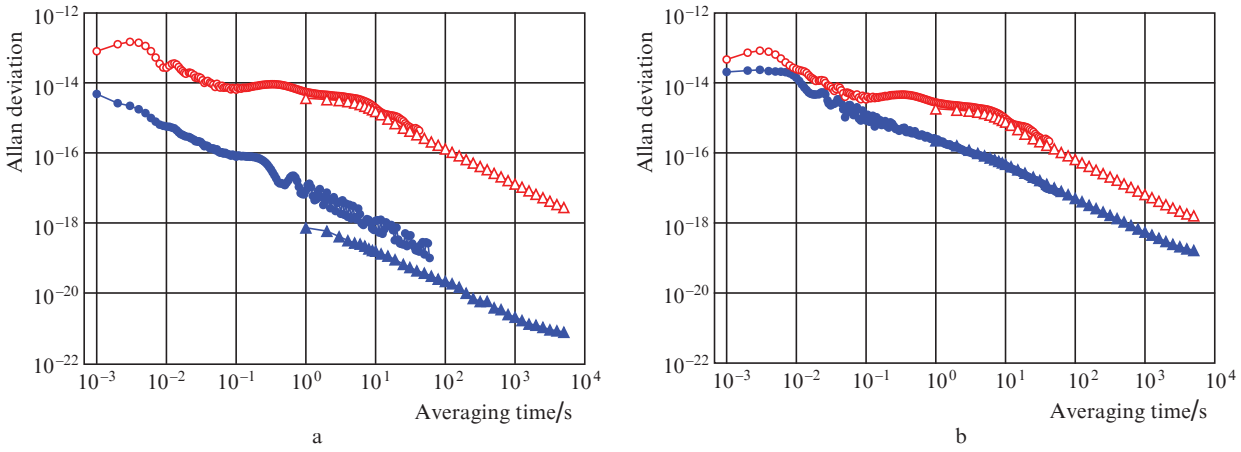

Figure 3. Dependences of the Allan deviation on the averaging time for (a) inloop and (b) remote signals without (open symbols) and with (closed symbols) noise compensation. Circles and triangles are the data obtained with counter windows of 1 ms and 1 s, respectively. Symbols are connected by lines for eye guidance.

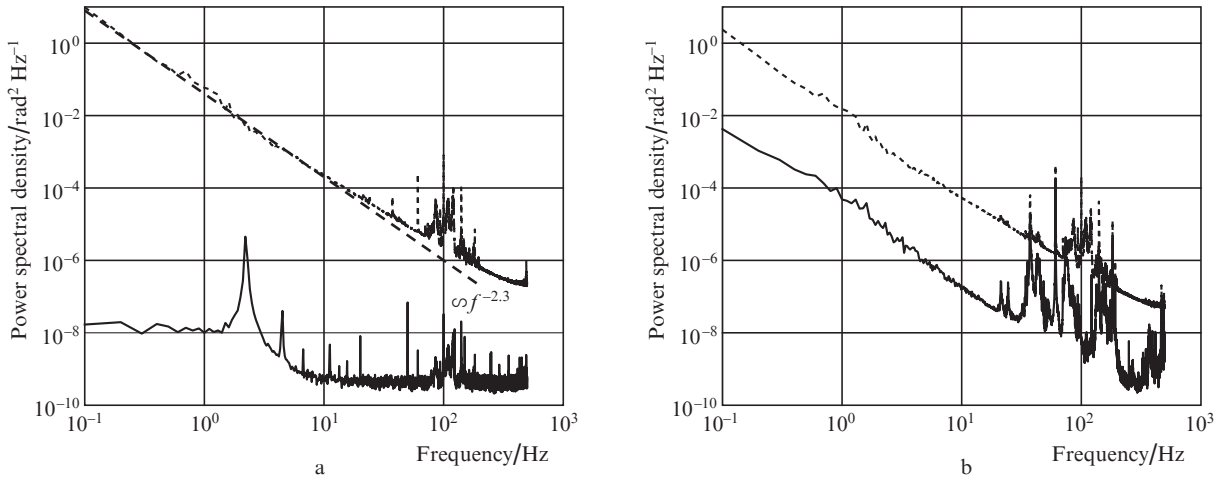

Figure 4. Power spectral density of phase noise, $S_\varphi(f)$, for the (a) inloop and (b) remote signals. The upper dotted curves correspond to the case without noise compensation, and the lower solid curves correspond to noise compensation. The dashed line in panel (a) is an approximation of low-frequency data by a power-law dependence $f^{-2.3}$.

laboratory ventilation system is approximately 0.1 m/s, we obtain $C_n = 2 \times 10^{-13}$ m$^{-2/3}$. In the frequency range of 10–500 Hz the dependence becomes flatter and tends to take the form of f^{-1}. The frequency range from 40 to 200 Hz contains resonance peaks, which may be due to mirror jitter and optical table rockings.

The power spectral density for an inloop signal with compensated noise is almost constant in the ranges of 0.1–2 Hz, 8–40 Hz, and 150–500 Hz; this fact indicates the dominance of white phase noise. The noise in the range of 3–8 Hz is similar to white frequency noise. One can see well resonances at frequencies of about 2 Hz and in the range of 40–150 Hz. The noise spectrum for a remote signal with active noise compensation differs significantly from that of the inloop signal: it has (i) a much larger amplitude and (ii) another character. There are resonances in the frequency range of 20–500 Hz, and the spectral shape in the range of 0.1–20 Hz is similar to that for the noise of unstabilised signals. A possible reason is the presence of optical path portions, which are uncommon for the inloop and remote signals; in particular, the large (about 0.5 m) distance from the splitting point to the photodiode, which is passed by the radiation arriving at the remote user (see Fig. 1), and the local interferometer forming an inloop beat signal. Isolation and thermal stabilisation of the residence region of local interferometer should reduce its influence. For the same reason, the vibrations across the beam axis of the optical table part with a console for mounting a cube splitting off a part of remote signal and a mirror reflecting the beam back (see Fig. 1) may contribute to the instability of remote signal, because the beam forming the inloop signal and, correspondingly, the error signal in the feedback loop is not reflected from the cube plane. However, it should be noted that the sensitivity to mirror motions along the beam axis is reduced in this scheme. The mirror-introduced noises are detected in the inloop signal and compensated by the feedback loop, being actually imprinted into the transferred radiation frequency. The signal arriving at the remote user is not reflected from this mirror; however, it is reflected from the cube plane at an angle of 45°; therefore, the noises due to the motions along the beam axis are compen-

sated for. Furthermore, we are planning to study this feature in more detail and improve the remote-signal characteristics.

In continuation of this study we are going to increase the link length to 500 m and use an unmanned aerial vehicle with a mirror fixed on it as a moving receiver model.

4. Conclusions

The frequency signal transfer via a free-space 5-m-long air link was investigated. The noise introduced by the link into the signal is determined by the influence of atmospheric turbulence, and its spectrum is described by the function $f^{-2.3}$. The deviations from the Kolmogorov theory can be explained by imperfection of the model, which suggests validity of the Taylor hypothesis and implies constant air velocity [13]; therefore, it cannot take into account all possible thermal and mechanical effects in air flows. The phase-noise compensation system makes it possible to reduce the link contribution to the transferred signal instability and error to a level of several parts of 10^{-19} after 5000-s averaging; thus, the link can be used to compare transported frequency standards.

Acknowledgements. This work was supported by the Russian Science Foundation (Grant No. 19-72-10166).

References

1. Riehle F. *Nat. Photonics*, **11**, 25 (2017).
2. Lewandowski, W., Arias, E.F. *Metrologia*, **48**, 219 (2011).
3. Mehlstäubler T.E., Grosche G., Lisdat C., et al. *Rep. Progr. Phys.*, **81**, 064401 (2018).
4. Clivati C., Costanzo G.A., Frittelli M., et al. *IEEE Trans. Ultrason. Ferroelectr. Freq. Control*, **62** (11), 1907 (2015).
5. Delva P., Lodewyck J., Bilicki S., et al. *Phys. Rev. Lett.*, **118**, 221102 (2017).
6. Wcisło P., Ablewski P., Beloy K., et al. *Sci. Adv.*, **4** (12), 1 (2018).
7. Oelker E., Hutson R.B., Kennedy C.J., et al. *Nat. Photonics*, **13**, 714 (2019).
8. Brewer S.M., Chen J.-S., Hankin A.M., et al. *Phys. Rev. Lett.*, **123**, 033201 (2019).
9. Fujieda M., Piester D., Gotoh T., et al. *Metrologia*, **51**, 253 (2014).
10. Droste S., Udem T., Holzwarth R., Hänsch T.W. *Comptes Rendus Physique*, **16** (5), 524 (2015).
11. Zhang H., Wu G., Li H., et al. *IEEE Photonics J.*, **8** (5), 1 (2016).
12. Samain E., Exertier P., Courde C., et al. *Metrologia*, **52**, 423 (2015).
13. Sinclair L.C., Giorgetta F.R., Swann W.C., et al. *Phys. Rev. A*, **89**, 023805 (2014).
14. Bergeron H., Sinclair L.C., Swann W.C., et al. *Nat. Commun.*, **10**, 1819 (2019).
15. Gozzard D.R., Schediwy S.W., Stone B., et al. *Phys. Rev. Appl.*, **10**, 024046 (2018).
16. Swann W.C., Sinclair L.C., et al. *Appl. Opt.*, **56**, 9406 (2017).
17. Fried D.L. *Proc. IEEE*, **55**, 57 (1967).
18. Wright M.W., Morris J.F., Kovalik J.M., et al. *Opt. Express*, **23**, 33705 (2015).
19. Golovizin A., Fedorova E., Tregubov D., et al. *Nat. Commun.*, **10**, 1724 (2019).
20. Semerikov I.A., Khabarova K.Yu., Zalivako I.V., et al. *Bull. Lebedev Phys. Inst.*, (45), 337 (2018) [*Kratk. Soobshch. Fiz. FIAN*, (11), 14 (2018)].
21. Sutyrin D.V., Berdasov O.I., Antropov S.Yu., et al. *Quantum Electron.*, **49**, 199 (2019) [*Kvantovaya Elektron.*, **49**, 199 (2019)].
22. Kudeyarov K.S., Vishnyakova G.A., Khabarova K.Yu., Kolachevsky N.N. *Laser Phys.*, **28**, 105103 (2018).
23. Williams P., Swann W.C., Newbury N.R. *J. Opt. Soc. Am. B*, **25** (8), 1284 (2008).
24. Khabarova K.Yu., Kudeyarov K.S., Vishnyakova G.A., Kolachevsky N.N. *Quantum Electron.*, **47**, 794 (2017) [*Kvantovaya Elektron.*, **47**, 794 (2017)].
25. Koller S.B., Grotti J., Vogt St., et al. *Phys. Rev. Lett.*, **118** (7), 073601 (2017).